HHS Public Access

Author manuscript

J Urol. Author manuscript; available in PMC 2022 May 09.

Published in final edited form as:

J Urol. 2015 October ; 194(4): 957–965. doi:10.1016/j.juro.2015.04.075.

Prostate Cancer Volume Estimation by Combining Magnetic Resonance Imaging and Targeted Biopsy Proven Cancer Core Length: Correlation with Cancer Volume

Toru Matsugasumi, **Eduard Baco**, **Suzanne Palmer**, **Manju Aron**, **Yoshinobu Sato**, **Norio Fukuda**, **Evren Süer**, **Jean-Christophe Bernhard**, **Hideo Nakagawa**, **Raed A. Azhar**, **Inderbir S. Gill**[*], **Osamu Ukimura**[†,‡]

USC Institute of Urology (TM, EB, ES, JCB, HN, RAA, ISG, OU) and Departments of Radiology (SP) and Pathology (MA), Keck School of Medicine, University of Southern California, Los Angeles, California, Department of Urology, Kyoto Prefectural University of Medicine (TM, HN), Kyoto and Imaging-based Computational Biomedicine Laboratory, Graduate School of Information Science, Nara Institute of Science and Technology (YS, NF), Nara, Japan, and Urology Department, King Abdulaziz University (RAA), Jeddah, Saudi Arabia

Abstract

Purpose: Multiparametric magnetic resonance imaging often underestimates or overestimates pathological cancer volume. We developed what is to our knowledge a novel method to estimate prostate cancer volume using magnetic resonance/ultrasound fusion, biopsy proven cancer core length.

Materials and Methods: We retrospectively analyzed the records of 81 consecutive patients with magnetic resonance/ultrasound fusion, targeted biopsy proven, clinically localized prostate cancer who underwent subsequent radical prostatectomy. As 7 patients each had 2 visible lesions on magnetic resonance imaging, 88 lesions were analyzed. The dimensions and estimated volume of visible lesions were calculated using apparent diffusion coefficient maps. The modified formula to estimate cancer volume was defined as the formula of vertical stretching in the anteroposterior dimension of the magnetic resonance based 3-dimensional model, in which the imaging estimated lesion anteroposterior dimension was replaced by magnetic resonance/ultrasound targeted, biopsy proven cancer core length. Agreement of pathological cancer volume with magnetic resonance estimated volume or the novel modified volume was assessed using a Bland-Altman plot.

Results: Magnetic resonance/ultrasound fusion, biopsy proven cancer core length was a stronger predictor of the actual pathological cancer anteroposterior dimension than magnetic resonance estimated lesion anteroposterior dimension ($r = 0.824$ vs 0.607, each $p < 0.001$). Magnetic resonance/ultrasound targeted, biopsy proven cancer core length correlated with pathological cancer volume ($r = 0.773$, $p < 0.001$). The modified formula to estimate cancer volume demonstrated a stronger correlation with pathological cancer volume than with magnetic

[*]Financial interest and/or other relationship with EDAP.

[‡]Financial interest and/or other relationship with SonaCare Medical.

[†]Correspondence: USC Institute of Urology, University of Southern California, 1441 Eastlake Ave., Suite 7416, Los Angeles, California 90089 (telephone: 323-865-3700; FAX: 323-865-0120; ukimura@usc.edu).

resonance estimated volume (r = 0.824 vs 0.724, each p <0.001). Agreement of modified volume with pathological cancer volume was improved over that of magnetic resonance estimated volume on Bland-Altman plot analysis. Predictability was more enhanced in the subset of lesions with a volume of 2 ml or less (ie if spherical, the lesion was approximately 16 mm in diameter).

Conclusions: Combining magnetic resonance estimated cancer volume with magnetic resonance/ultrasound fusion, biopsy proven cancer core length improved cancer volume predictability.

Keywords

prostatic neoplasms; biopsy; magnetic resonance imaging; tumor burden; prognosis

MULTIPARAMETRIC MRI is a highly accurate method to visualize clinically significant cancer.[1,2] Index cancer volume determined by MRI may be helpful to plan treatment, particularly to identify tumor margins for image guided focal therapy and select better candidates for active surveillance.[3] DWI is sensitive to visualization of tissue structures at the microscopic level and ADC calculated from DWI was reported to be promising to determine cancer volume.[4–8]

However, even combinations of all mp-MRI sequences often underestimate or overestimate the pathological volume of a cancer. Such inaccurate measurements have estimated moderate correlation coefficients that vary from 0.55 to 0.90 based on PCV and MRI measured lesion volume.[1,3,5–10] Therefore, improved precise estimates of cancer volume may need to consider additional parameters, which may allow for adjustments or modifications to MRI data to match more closely the actual pathological volume of a cancer.[7] Several reports have suggested that targeted biopsies using mp-MRI provide significantly greater cancer core length and higher Gleason scores for MR visible lesions than random biopsies.[11–13] They may enhance accurate risk stratification through improved cancer characterization.[14–16]

Accordingly we hypothesized that combining MRI measured volume with targeted biopsy proven cancer core length may improve our ability to estimate cancer volume. In this study using RP as the reference standard we first evaluated the accuracy of mp-MRI to estimate cancer volume in each patient in whom cancer was confirmed by MR/US fusion targeted biopsy. We then further identified a novel modification formula to improve the estimated cancer volume combined with MRI and targeted biopsy proven cancer core length, and compared that estimate with the MRI based estimation.

MATERIALS AND METHODS

This study was approved by the local institutional review board. From 2010 to 2014 we enrolled 81 consecutive patients with increased PSA who sequentially underwent certain procedures, including 1) prebiopsy MRI, 2) MR/US fusion targeted biopsy of a MRI suspicious lesion and 3) robot-assisted RP as primary treatment. Figure 1 shows a flow chart of patients in this study. The median interval between prebiopsy MRI and biopsy was 3 days (range 0 to 116), and between MRI and RP it was 52 days (range 13 to 171). The

table lists the characteristics of the 81 patients. Since 7 patients each had 2 visible cancers on MRI, a total of 88 visible lesions were analyzed.

MRI was performed using a 3 Tesla MR-750 MRI scanner (GE®) and a 16-channel phased array body coil. T2w and DWI sequences were used to generate ADC maps with or without dynamic contrast enhanced MRI. Before biopsy MRI was assessed by a radiologist (SP) who had experience with reviewing prostate MR in more than 150 cases. All MR/US fusion targeted biopsies were performed with the patient under local anesthesia by an experienced urologist (OU) who had performed more than 150 cases with the Urostation®.

All RP specimens were assessed by the modified Stanford technique. The gland was cut perpendicularly every 3 to 5 mm in sections from apex to base. Both ends of the 5 to 8 mm distal section of the apex and base were horizontally coned and amputated. Each formalin fixed, paraffin embedded slice was stained with hematoxylin and eosin. Step section cancer maps from apex to base were assessed.

Cancer Volume and Contact Length Measurement on MRI and in RP Specimens

Identification by measuring the suspect lesion in ADC and/or T2w sequences was performed manually by a radiologist (SP) and a urologist (OU) experienced with prostate MRI. On the ADC axial scan showing the maximum area of the MR visible lesion the AP dimension (height in mm) and the axial transverse dimension (width in mm) were obtained. The craniocaudal dimension (length in mm) was calculated by the formula, 3 mm × (n + 1), where n is equal to the number of ADC slices containing the visible lesion. The inclusion of the slice with equivocal visibility of the lesion in the ADC axial scan was confirmed by visibility of the lesion on the sagittal or the coronal T2w image. To determine MCV at the largest perpendicular diameter we applied the ellipsoid volume formula, height × width × length × 0.5.

Of the 88 lesions the PI-RADS (Prostate Imaging Reporting and Data System) score was 5 in 9 (10.2%), 4 in 54 (61.4%) and 3 in 25 (28.4%). On the pathological slide showing the maximum area of the targeted biopsy proven cancer the AP dimension (height in mm) and the axial transverse dimension (width in mm) were determined. The craniocaudal dimension (length in mm) was calculated using the formula, slice thickness × (n + 1), where n represents the number of slides containing the lesion. Each PCV was calculated by the simplified 3D estimation method of the ellipsoid formula, height × width × length 0.5, without a shrinkage correlation as described by Perera et al.[17]

Development of Prostate and Biopsy Proven Lesion 3D Model

Segmentation of the prostate and cancer models was performed on MRI (DWI-ADC/T2w) images manually using computer software. Digitized 3D prostate data and each biopsy trajectory were acquired during prostate biopsy with a 3D5–9EK 3D end fire TRUS probe (Samsung Medison America, Cypress, California) using a Urostation external computer workstation. At biopsy we inked the distal end of each core to orient the biopsy specimen. Thus, the pathologist could precisely document the extent and location of cancer in the biopsy core (fig. 2, A).

We digitally color coded cancer regions red and benign regions green on each biopsy core. By image fusing the MRI data with the 3D TRUS coordinates of the recorded needle trajectory we constructed a 3D model of the prostate and a 3D model of the MR estimated lesion with overlaid biopsy trajectories that color coded the cancer (red) and benign (green) regions. Finally, a new modified 3D cancer model was created. This was done first by replacing the MR estimated lesion AP dimension with the MR/US targeted biopsy proven cancer core length. According to the overlaid red color coded biopsy trajectory on the original MRI based 3D model we finally used affine transformation to create the new modified 3D model with vertical stretching of the AP dimension of the original MRI based 3D model (fig. 2, B).

Statistical Analysis

Descriptive statistics of the patient, MRI and pathological characteristics were assessed for 81 men and 88 MR visible lesions. Logistic regression analysis was done to define the correlation between PCV and estimated volume. Agreement of PCV with MCV or modified volume was assessed using a Bland-Altman plot. All statistical analyses were performed with SPSS® Statistics, version 21.0 with results considered significant at $p < 0.05$.

RESULTS

Regression analysis revealed that the Spearman correlation coefficient (r) between PCV and MCV was 0.724 ($p < 0.001$, fig. 3, A). MR/US fusion biopsy proven cancer core length was a better predictor of the actual pathological cancer AP dimension than the MR estimated lesion AP dimension ($r = 0.824$ vs 0.607, each $p < 0.001$, fig. 3, B and C). MR/US targeted biopsy proven cancer core length correlated with PCV ($r = 0.773$, $p < 0.001$, fig. 3, D).

When replacing the MR estimated cancer AP dimension with the MR/US fusion biopsy proven cancer core length, the modified estimation of cancer volume significantly improved (fig. 4, A). The enhanced predictability was especially effective in the subset of lesions with a cancer volume of less than 2 ml (ie if it was spherical, it was approximately 16 mm in diameter) ($r = 0.847$, $p < 0.001$, fig. 4, B and C).

Agreement between modified volume and PCV outperformed that between MCV and PCV as shown in the Bland-Altman plot (fig. 5, A). Agreement was represented by closer distribution of the plots to the red line (mean difference) in the relation between modified volume and PCV than that between MCV and PCV. Agreement between modified volume and PCV was more obvious in the subsets with a cancer volume of less than 2 ml (fig. 5, B). When analyzing the rate with the stronger agreement using the Bland-Altman approach, ie regarding the rate of the plots in the distribution range of within $\pm 0.5 \times SD$, the rate improved from only 26.7% of the MCV (19 of 71 lesions) to 35.2% (25 of 71) of the modified volume (fig. 5, B).

DISCUSSION

Our study demonstrates that cancer volume estimation with only DWI-ADC as a parameter significantly correlated with PCV but still significantly overestimated and underestimated

PCV. MR/US targeted biopsy proven cancer core length significantly correlated with MR estimated lesion AP dimension and correlated with PCV. Thus, we developed a more accurate estimation formula to predict cancer volume with vertical stretching of the MR estimated AP dimension of the original MRI based 3D model according to the MR/US fusion, targeted biopsy proven cancer core length. When applying our newly developed modified formula to estimate cancer volume, the predictability of cancer volume significantly improved, especially for cancer volumes less than 2 ml in which the AP diameter of the lesion likely corresponded with MR/US fusion targeted biopsy core length (less than 17 mm).

Recent studies using 3D surgical models to visualize the cancer location beyond the surgical view may enhance outcomes in robot-assisted RP.[18–20] Furthermore, there is increasing interest in minimally invasive, targeted focal therapies to only treat the biopsy proven visible lesion within a particular safety margin.[7,21–25] Multiple studies have shown that the index lesions may determine the biological driver of a prostate malignancy in a given patient.[26–28] Targeted focal therapy is supported by the hypothetical concept of controlling/curing the index prostate cancer with preservation of the remaining prostate, urethral sphincter and neurovascular bundles, thereby reducing treatment related side effects.[21–23]

To achieve reliable ablation of the index cancer imaging should ideally define the absolute microscopic margins of the index cancer or reliably determine the additional safety margins to be ablated around the image visible margins of the index cancer. mp-MRI has the greatest potential to determine cancer margins and, thus, the pathological volume of clinically important cancer. However, previous reports as well as our study have demonstrated that mp-MRI is not yet able to reliably predict cancer volume because of significant over-estimations or underestimations of PCV.[3,5–10]

Based on the reports by Cornud[7] and Donati[8] et al, which proved that DWI-ADC is the best method to predict actual tumor volume, we applied DWI-ADC to estimate PCV. Interestingly multiple regression analysis revealed that DWI-ADC estimated cancer volume ($p < 0.001$) and MRI targeted biopsy proven cancer core length ($p < 0.003$) were significant independent predictors of PCV ($r = 0.796$, $F = 44.4$, $p < 0.001$).

Importantly our subsequent regression analysis revealed that MR/US fusion biopsy proven cancer core length is a better predictor of the actual pathological cancer AP dimension than the MR estimated lesion AP dimension. When replacing the MR estimated lesion AP dimension with MR/US fusion biopsy proven cancer core length, the modified estimation of cancer volume significantly improved. Notably the enhanced predictability worked best (ie further improvement to $r = 0.847$, $p < 0.001$) in the subset of lesions with a cancer volume of less than 2 ml (ie if it was spherical, it was approximately 16 mm in diameter). This finding was confirmed on Bland-Altman plot analysis.

Interestingly these results indicate that when the cancer dimension is within 16 mm, based on the fact that an approximately 16 mm length of tissue corresponds exactly to a tissue sampling notch of the biopsy needle, the modified cancer volume estimation technique with integration between the MR visible lesion and the targeted biopsy proven cancer core length

works well. On the other hand, when the lesion is larger than 2 ml (with a diameter greater than 16 mm if spherical), the novel modification of the cancer volume estimation is less accurate. When considering the threshold for clinically significant cancer, this modified estimation method is applicable for typical cancers with a volume of 0.5 ml (with a 10 mm dimension if spherical) or greater.

Our study has limitations. 1) The AP axis of the prostate MRI is not necessarily completely matched to the direction of the biopsy proven cancer core length. Because the AP axis of a body in a MRI scanner bed generally serves as the AP axis of the MRI, the direction of the AP axis of the prostate against the posterior surface of the prostate varies case by case. In fact, the direction of the biopsy with end fire TRUS against the posterior surface of the prostate also varies in each sampling based on the deformation of the prostate and the angulation of the probe. As such, we argue that the AP axis of the MR lesion is similar to the direction of the TRUS biopsy but not necessarily matched to the direction of the biopsy. However, importantly our data suggest that although MRI likely underestimates or overestimates the size of the cancer, the MR/US fusion targeted biopsy proven cancer core length likely represents the reality of the AP dimension of the cancer, resulting in better prediction of cancer volume than the MRI estimated AP dimension. 2) Our cutting procedure for RP specimens was not prospectively designed using the mold excision or meat slicer technique to achieve consistency. Due to the retrospective nature of this study a precise definition of the craniocaudal dimension in step sections of RP specimens was challenging because of several factors, including differences in section angle and thickness, prostate deformation and/or loss of volume during pathological processing. As such the ellipsoid formula with variable slice thickness may have limitations as the ideal reference standard of volume analysis. 3) We did not separately evaluate each MRI sequence for its ability to predict cancer volume. Instead our study was based on previous reports that among all MRI sequences DWI likely provides the highest ability to identify prostate cancer. 4) Because the MRI field was created by a 3 Tesla body coil, accuracy may be inferior to that achieved with an endorectal coil. 5) The modified volume estimation formula works well for cancer volumes 2 ml or less, which corresponds to an approximately 16 mm sphere. However, its estimation for greater foci may be less accurate. 6) As in the 3D model, our study only improved 1 dimension of the AP axis. Thus, further effort is necessary to improve the total underestimation or overestimation in other dimensions.

Interestingly Le Nobin et al recently reported that MRI underestimates histologically determined tumor boundaries but simulated treatment volume based on a 9 mm image guided focal ablation margin as the optimal ablation margin achieved complete histological tumor destruction in 100% of patients.[25] It would require further research to determine the optimal method to determine the treatment margin during image guided focal ablation. For future research possible options may include 1) setting up such a 9 mm margin around MR visible lesions in all cases with consideration of the worst scenario or 2) making an effort toward individualized correction of MRI underestimation of the lesion with an additional parameter to better represent reality in the tissue, such as the targeted biopsy proven cancer core length.

Our approach is based on the result that biopsy proven cancer core length more likely represents the real size in the tissue than the MRI visible size of the lesion. In our study we applied the transrectal approach. However, this series may be applicable to the transperineal approach, that is to propose modification of the MRI craniocaudal dimension by replacing the transperineal biopsy proven cancer core length.

CONCLUSIONS

There are significant but limited correlations between PCV and MCV. MR/US targeted biopsy proven cancer core length was a stronger predictor of the actual pathological cancer AP dimension than the MR estimated lesion AP dimension and it correlated with PCV. Therefore, we developed a modified volume estimation formula using MR/US fusion targeted biopsy proven cancer core length. Predictability (agreement between modified volume and PCV) was enhanced, especially in cases with cancer volumes less than 2 ml (ie maximum lesion diameter 16 mm or less).

Acknowledgments

Study received local institutional review board approval.

Abbreviations and Acronyms

3D	3-dimensional
ADC	apparent diffusion coefficient
AP	anteroposterior
DWI	diffusion weighted imaging
MCV	MRI estimated cancer volume
mp	multiparametric
MR	magnetic resonance
MRI	magnetic resonance imaging
MR/US	magnetic resonance/ultrasound
PCV	pathological cancer volume
PSA	prostate specific antigen
RP	radical prostatectomy
T2w	T2-weighted
TRUS	transrectal ultrasound

REFERENCES

1. Villers A, Puech P, Mouton D et al. : Dynamic contrast enhanced, pelvic phased array magnetic resonance imaging of localized prostate cancer for predicting tumor volume: correlation with radical prostatectomy findings. J Urol 2006; 176: 2432. [PubMed: 17085122]
2. Hoeks CM, Barentsz JO, Hambrock T et al. : Prostate cancer: multiparametric MR imaging for detection, localization, and staging. Radiology 2011; 261: 46. [PubMed: 21931141]
3. Turkbey B, Mani H, Aras O et al. : Correlation of magnetic resonance imaging tumor volume with histopathology. J Urol 2012; 188: 1157. [PubMed: 22901591]
4. Charles-Edwards EM and deSouza NM: Diffusion-weighted magnetic resonance imaging and its application to cancer. Cancer Imaging 2006; 6: 135. [PubMed: 17015238]
5. Mazaheri Y, Hricak H, Fine SW et al. : Prostate tumor volume measurement with combined T2-weighted imaging and diffusion-weighted MR: correlation with pathologic tumor volume. Radiology 2009; 252: 449. [PubMed: 19703883]
6. Isebaert S, Van den Bergh L, Haustermans K et al. : Multiparametric MRI for prostate cancer localization in correlation to whole-mount histopathology. J Magn Reson Imaging 2013; 37: 1392. [PubMed: 23172614]
7. Cornud F, Khoury G, Bouazza N et al. : Tumor target volume for focal therapy of prostate cancer–does multiparametric magnetic resonance imaging allow for a reliable estimation? J Urol 2014; 191: 1272. [PubMed: 24333516]
8. Donati OF, Afaq A, Vargas HA et al. : Prostate MRI: evaluating tumor volume and apparent diffusion coefficient as surrogate biomarkers for predicting tumor Gleason score. Clin Cancer Res 2014; 20: 3705. [PubMed: 24850842]
9. Coakley FV, Kurhanewicz J, Lu Y et al. : Prostate cancer tumor volume: measurement with endorectal MR and MR spectroscopic imaging. Radiology 2002; 223: 91. [PubMed: 11930052]
10. Junker D, Sch€afer G, Kobel C et al. : Comparison of real-time elastography and multiparametric MRI for prostate cancer detection: a whole-mount step-section analysis. AJR Am J Roentgenol 2014; 202: W263. [PubMed: 24555623]
11. Kasivisvanathan V, Dufour R, Moore CM et al. : Transperineal magnetic resonance image targeted prostate biopsy versus transperineal template prostate biopsy in the detection of clinically significant prostate cancer. J Urol 2013; 189: 860. [PubMed: 23063807]
12. Delongchamps NB, Peyromaure M, Schull A et al. : Prebiopsy magnetic resonance imaging and prostate cancer detection: comparison of random and targeted biopsies. J Urol 2013; 189: 493. [PubMed: 22982424]
13. Pokorny MR, de Rooij M, Duncan E et al. : Prospective study of diagnostic accuracy comparing prostate cancer detection by trans-rectal ultrasound-guided biopsy versus magnetic resonance (MR) imaging with subsequent MR-guided biopsy in men without previous prostate biopsies. Eur Urol 2014; 66: 22. [PubMed: 24666839]
14. Bjurlin MA, Meng X, Le Nobin J et al. : Optimization of prostate biopsy: the role of magnetic resonance imaging targeted biopsy in detection, localization and risk assessment. J Urol 2014; 192: 648. [PubMed: 24769030]
15. Baco E, Ukimura O, Rud E et al. : Magnetic resonance imaging-transrectal ultrasound image-fusion biopsies accurately characterize the index tumor: correlation with step-sectioned radical prostatectomy specimens in 135 patients. Eur Urol 2015; 67: 787. [PubMed: 25240973]
16. Ukimura O, Marien A, Palmer S et al. : Trans-rectal ultrasound visibility of prostate lesions identified by magnetic resonance imaging increases accuracy of image-fusion targeted biopsies. World J Urol 2015; Epub ahead of print.
17. Perera M, Lawrentschuk N, Bolton D et al. : Comparison of contemporary methods for estimating prostate tumour volume in pathological specimens. BJU Int 2014; 113: 29. [PubMed: 24053510]
18. Baco E, Rud E, Vlatkovic L et al. : Predictive value of magnetic resonance imaging determined tumor contact length for extra-capsular extension of prostate cancer. J Urol 2014; 193: 466. [PubMed: 25150643]

19. Ukimura O, Aron M, Nakamoto M et al. : Three-dimensional surgical navigation model with TilePro display during robot-assisted radical prostatectomy. J Endourol 2014; 28: 625. [PubMed: 24450285]
20. Simpfendörfer T, Baumhauer M, Müller M et al. : Augmented reality visualization during laparoscopic radical prostatectomy. J Endourol 2011; 25: 1841. [PubMed: 21970336]
21. Ahmed HU, Hindley RG, Dickinson L et al. : Focal therapy for localised unifocal and multifocal prostate cancer: a prospective development study. Lancet Oncol 2012; 13: 622. [PubMed: 22512844]
22. Bahn D, Abreu AC, Gill IS et al. : Focal cryotherapy for clinically unilateral low-intermediate risk prostate cancer in 73 men with median 3.7-year follow-up. Eur Urol 2012; 62: 55. [PubMed: 22445223]
23. Donaldson IA, Alonzi R, Barratt D et al. : Focal therapy: patients, interventions, and outcomes–a report from a consensus meeting. Eur Urol 2015; 67: 771. [PubMed: 25281389]
24. de Castro Abreu AL, Bahn D, Chopra S et al. : Real-time transrectal ultrasonography-guided hands-free technique for focal cryoablation of the prostate. BJU Int 2014; 114: 784. [PubMed: 24802231]
25. LeNobin J, Rosenkrantz AB, Villers A et al. : Image guided focal therapy for magnetic resonance imaging visible prostate cancer: defining 3-dimensional treatment margin based on magnetic resonance imaging histology co-registration analysis. J Urol 2015; 194: 364. [PubMed: 25711199]
26. Stamey TA, McNeal JE, Yemoto CM et al. : Biological determinants of cancer progression in men with prostate cancer. JAMA 1999; 281: 1395. [PubMed: 10217055]
27. Wise AM, Stamey TA, McNeal JE et al. : Morphologic and clinical significance of multifocal prostate cancers in radical prostatectomy specimens. Urology 2002; 60: 264. [PubMed: 12137824]
28. Noguchi M, Stamey TA, McNeal JE et al. : Prognostic factors for multifocal prostate cancer in radical prostatectomy specimens: lack of significance of secondary cancers. J Urol 2003; 170: 459. [PubMed: 12853799]

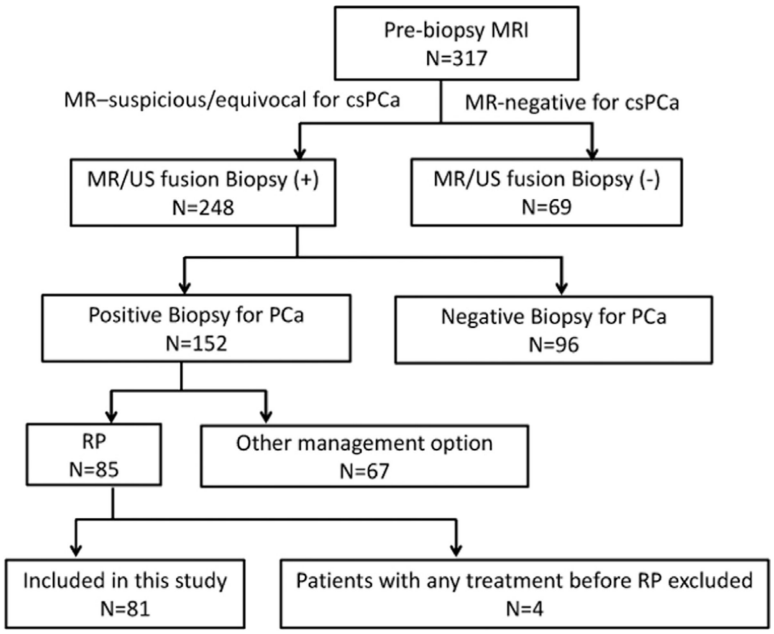

Figure 1.

Number of men included in study. *cs*, clinically significant. *PCa*, prostate cancer.

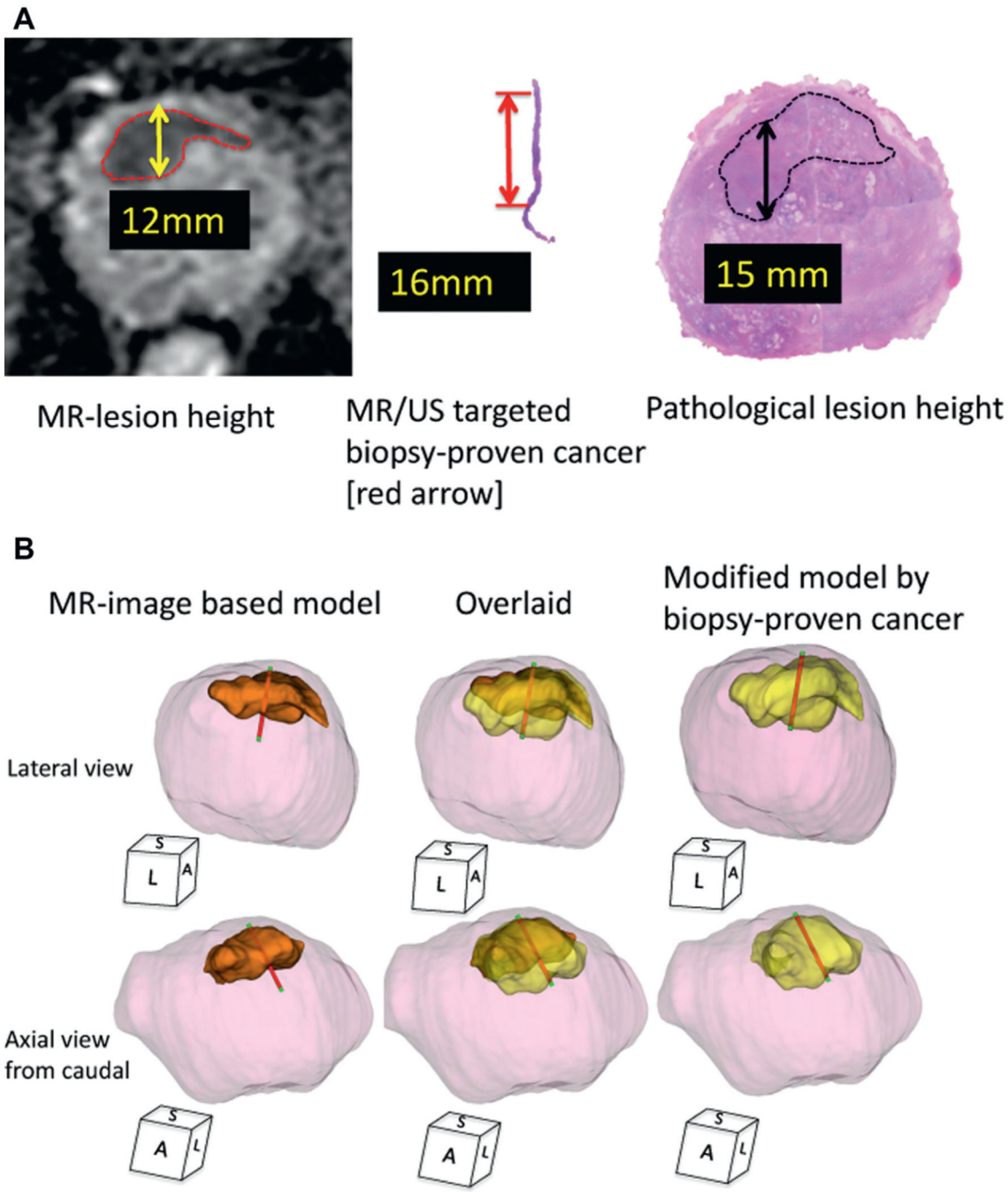

Figure 2.

Case presentation of MR visible lesion modification using MR/US fusion biopsy proven cancer core length. *A*, MR, targeted biopsy and prostatectomy data on 69-year-old man with PSA 7.4 ng/ml in whom prebiopsy MRI demonstrated PI-RAD level 5 suspicious lesion in anterior prostate. Height was 12 mm on DWI-ADC and MR/US image fusion targeted biopsy showed Gleason 3 + 4 with 16 mm core length. Subsequent robot-assisted RP revealed pathological T2c prostate cancer with dominant anterior cancer with maximum 15 mm anteroposterior lesion height. *B*, 3D tumor model, MRI based model and modified

model created by replacing MR estimated lesion height with MR/US targeted biopsy proven cancer core length and vertically stretching height of original MRI based 3D model according to cancer core length. Final PCV of this index lesion was 4.5 ml. Model of 3D MCV (orange area) was 2.5 ml (56%). Newly developed, modified MCV (yellow area) was 3.6 ml (80%). *Overlaid*, MR/US targeted biopsy trajectory overlay of both 3D models using documented digitalized coordinates obtained from real-time 3D TRUS tracking technology with Urostation. Red areas indicate pathologically proven cancer tissue. Green areas indicate benign tissue. *S*, sagittal. *L*, lateral. *A*, anterior.

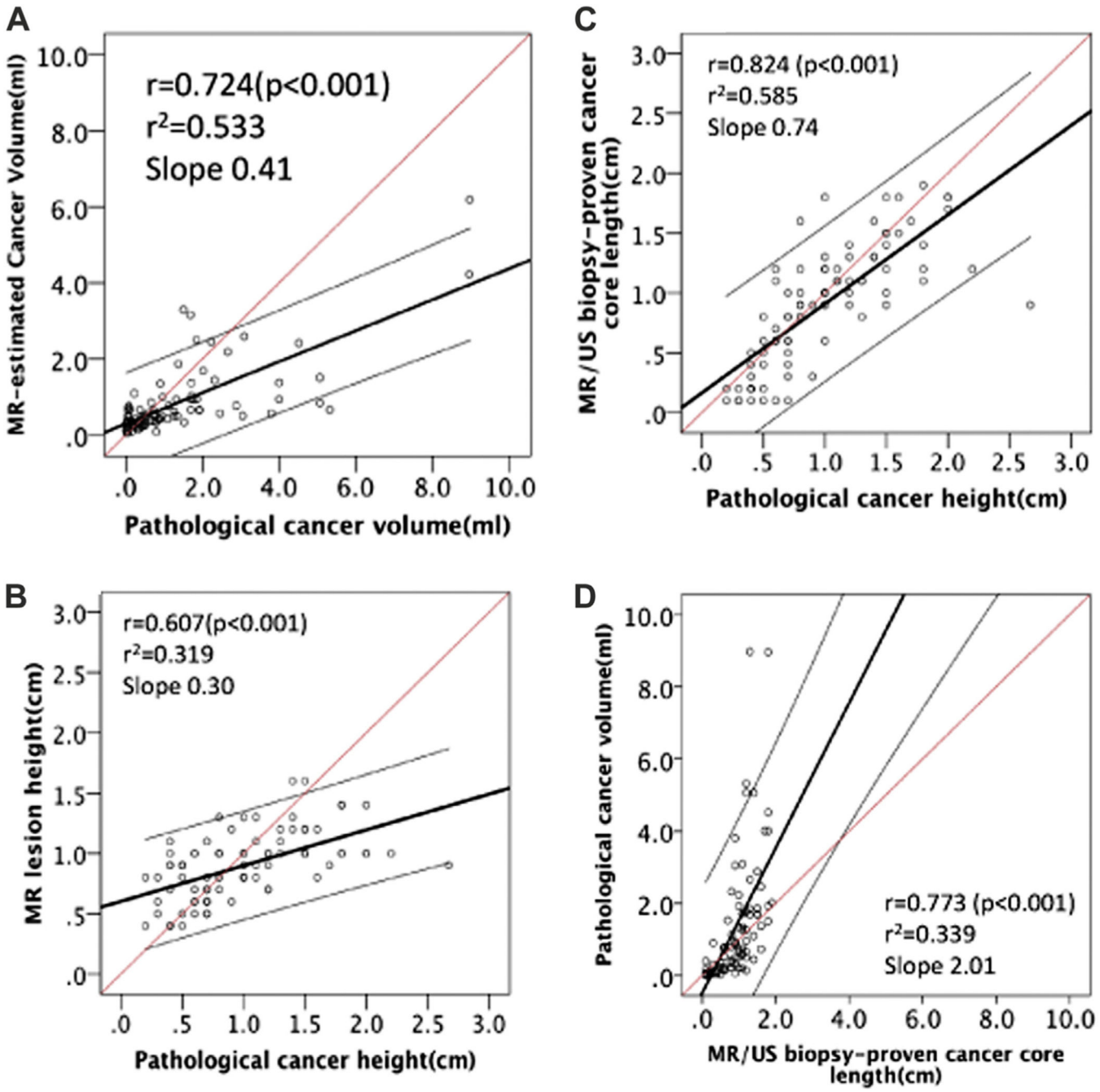

Figure 3.

A, MCV significantly correlated with PCV (r = 0.724, r^2 = 0.533, p <0.001). *B*, correlation between pathological cancer height (AP dimension) and MRI lesion height (AP dimension) (r = 0.607, r^2 = 0.319, slope 0.30, p <0.001). *C*, correlation between pathological cancer height (AP dimension) and MR/US biopsy proven cancer core length (r = 0.824, r^2 = 0.585, slope 0.74, p <0.001). *D*, correlation between PCV and MR/US biopsy proven cancer core length (r = 0.773, r^2 = 0.339, slope 2.01, p <0.001). Red line represents predicted ideal. Black line indicates identified line. Gray lines represent 95% CI.

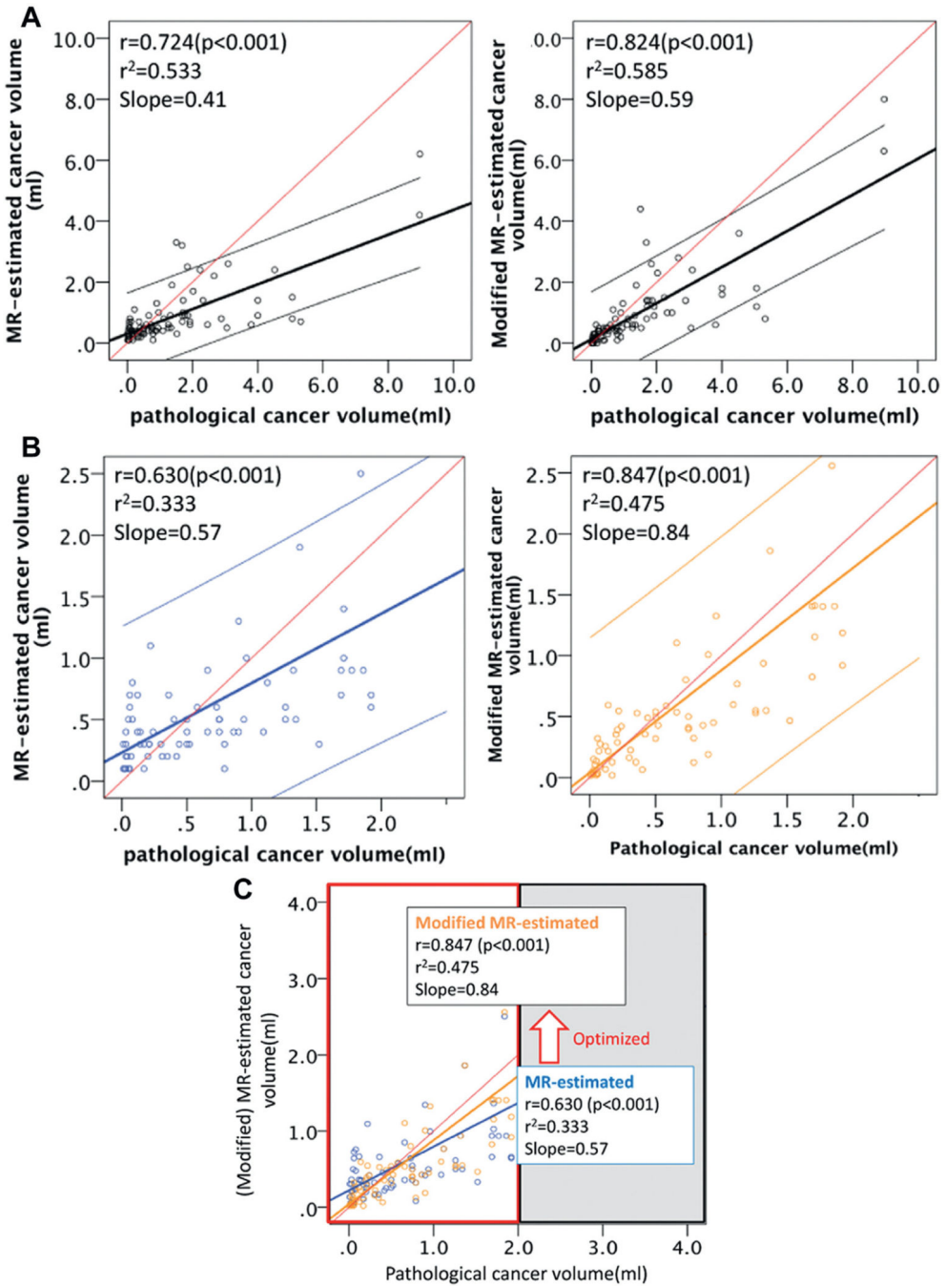

Figure 4.

Correlation of clinical variables with PCV on modification and subset analysis. *A*, in entire cohort of 88 lesions PCV significantly correlated with MCV (r = 0.724, r^2=0.533, slope 0.533, p <0.001) and modified MVC (r = 0.824, r^2=0.585, slope 0.59, p <0.001). *B*, on subset analysis of 71 cases of PCV less than 2.0 ml Spearman correlation of PCV and MCV was only 0.630 (r^2 = 0.333, slope 0.57, p <0.001), which was relatively lower. When estimation was modified by biopsy proven cancer core length, r improved to 0.847 (r^2 = 0.475, slope 0.84, p <0.001) compared to analysis of entire cohort of 88 cases. Reason for

improved predictability of cancer volume may be for cancer volumes less than 2 ml height of lesion most likely corresponded to biopsy core length, which was limited by biopsy sampling device to 16 mm or less. Note that volume of approximately 16 mm sphere is approximately 2 ml. *C*, improvement on subset analysis estimation for volumes less than 2 ml vs entire cohort. Optimization of new modification for cancer volume estimation improved from previous results (blue) to subsequent results (orange), especially in subgroup with PCV less than 2.0 ml. Red line indicates predicted ideal. Blue and orange lines represent identified lines.

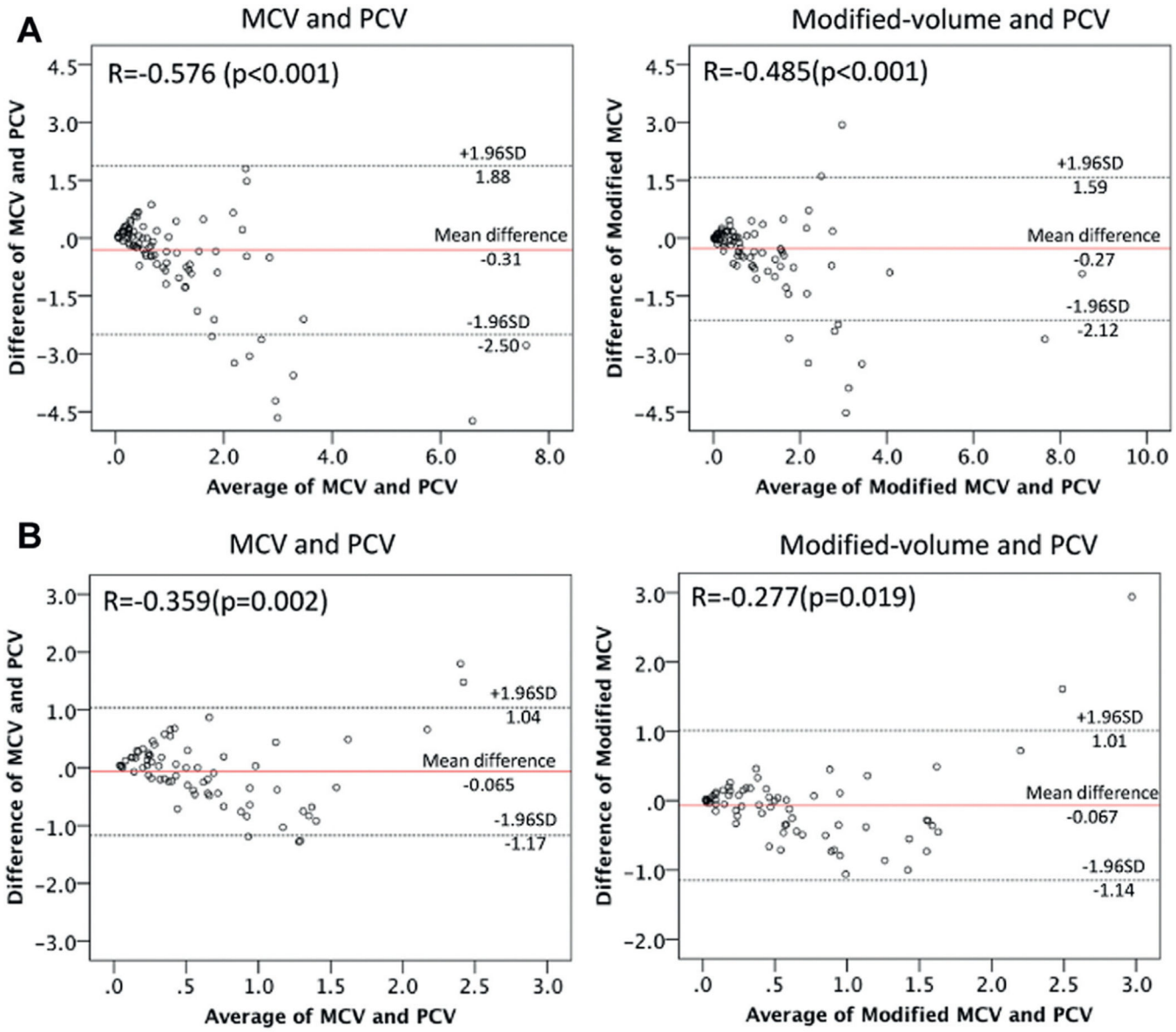

Figure 5.

Bland-Altman plot to assess agreement between 2 clinical measurement methods. *A*, in all 88 cases. *B*, in 71 cases with PCV less than 2 ml.

Characteristics of patients and pathological characteristics of MR/US biopsy proven cancers

No. pts/No. lesions	81/88*	
Median age (range)	64	(46—83)
Median ng/ml PSA (range)	7.4	(2.2—25.0)
Median ml pathological prostate vol (range)	44.8	(18.0—137.0)
No. clinical stage (%):		
cT1c	67	(82.7)
cT2a—c	14	(17.3)
No. pathological stage (%):		
pT2a, b	11	(13.6)
pT2c	49	(60.5)
pT3a	17	(21.0)
pT3b	4	(4.9)
No. Gleason score (%):		
3 + 3	21	(23.9)
3 + 4	48	(54.5)
4 + 3	9	(10.2)
4 + 4	2	(2.3)
3 + 5	4	(4.5)
4 + 5	4	(4.5)
No. Ca location (%):		
Peripheral zone	65	(73.9)
Transition zone	23	(26.1)
PCV (ml):		
Median (range)	0.75	(0.01—8.97)
No. less than 0.2 (%)	22	(25.0)
No. 0.2—less than 0.5 (%)	12	(13.6)
No. 0.5—less than 2.0 (%)	37	(42.0)
No. 2.0 or greater (%)	17	(19.3)
Median ml MCV (range)	0.5	(0.06—6.20)

*Seven patients each had 2 MR/US fusion targeted biopsy proven lesions.